KIF2 Is a New Microtubule-based Anterograde Motor That Transports Membranous Organelles Distinct from Those Carried by Kinesin Heavy Chain or KIF3A/B

Yasuko Noda, Reiko Sato-Yoshitake, Satoru Kondo, Masaomi Nangaku, and Nobutaka Hirokawa

Department of Anatomy and Cell Biology, Faculty of Medicine, University of Tokyo, Hongo, Tokyo 113, Japan

Abstract. Kinesin is known as a representative cytoskeletal motor protein that is engaged in cell division and axonal transport. In addition to the mutant assay, recent advances using the PCR cloning technique have elucidated the existence of many kinds of kinesin-related proteins in yeast, *Drosophila*, and mice. We previously cloned five different members of kinesin superfamily proteins (KIFs) in mouse brain (Aizawa, H., Y. Sekine, R. Takemura, Z. Zhang, M. Nangaku, and N. Hirokawa. 1992. *J. Cell Biol.* 119:1287–1296) and demonstrated that one of them, KIF3A, is an anterograde motor (Kondo, S., R. Sato-Yashitake, Y. Noda, H. Aizawa, T. Nakata, Y. Matsuura, and N. Hirokawa. *J. Cell Biol.* 1994. 125:1095–1107). We have now characterized another axonal transport motor, KIF2. Different from other KIFs, KIF2 is a central type motor, since its motor domain is located in the center of the molecule. Recombinant KIF2 exists as a dimer with a bigger head and plus-end directionally moves microtubules at a velocity of 0.47 ± 0.11 μm/s, which is two thirds that of kinesin's. Immunocytological examination showed that native KIF2 is abundant in developing axons and that it accumulates in the proximal region of the ligated nerves after a 20-h ligation. Soluble KIF2 exists without a light chain, and KIF2's associated-vesicles, immunoprecipitated by anti-KIF2 antibody, are different from those carried by existing motors such as kinesin and KIF3A. They are also distinct from synaptic vesicles, although KIF2 is accumulated in so-called synaptic vesicle fractions and embryonal growth cone particles. Our results strongly suggest that KIF2 functions as a new anterograde motor, being specialized for a particular group of membranous organelles involved in fast axonal transport.

NEURONS possess a highly polarized cytoarchitecture and transport system that enable them to perform their specialized functions. Especially within axons, each membrane or substrate is transported at the proper velocity and direction. Specialized markers have been used to identify many kinds of axonal transports, which can be roughly classified into several groups based on their velocities and directions (Grafstein and Forma, 1980; Dahlström et al., 1992). The variety of cross-bridge structures connecting vesicles and microtubules also supports the existence of a plural mechanism for axonal transport (Hirokawa et al., 1982, 1991).

Kinesin and cytoplasmic dynein are representative motors of anterograde and retrograde axonal transport, respectively (Vale et al., 1985; Brady et al., 1985; Paschal et al., 1987). To better understand possible involvement of other motor molecules, we previously searched for new ones and ultimately applied the PCR method to clone five kinesin-like molecules (kinesin superfamily proteins [KIFs][1] 1-5) using their homology with the kinesin motor domain (Aizawa et al., 1992), and subsequently demonstrated that one of them, KIF3A is an anterograde motor (Kondo et al., 1994).

KIF2, another superfamily member, has a unique structure in that its motor domain is located at the center of the molecule. To characterize this putative motor, we expressed KIF2 in a baculovirus system and then examined its biochemical behavior, molecule structure, and motor activity. Results indicate it functions as a plus-end-directed motor. In addition, we characterized KIF2's distribution and dynamics within ligated axons, as well as further purifying native molecules with their binding vesicles via the immunoprecipitation method; thereby demonstrating KIF2 to be another fast

Y. Noda and R. Sato-Yoshitake contributed equally to this study.

Address all correspondence to Prof. N. Hirokawa, Department of Anatomy and Cell Biology, Faculty of Medicine, University of Tokyo, 7-3-1 Hongo, Tokyo 113, Japan. Ph.: (81)3-3812-2111 (ext. 3326). Fax: (81) 3-5689-4856.

1. *Abbreviations used in this paper*: KHC, kinesin heavy chain; KIF, kinesin superfamily protein; PVDF, polyvinylidene defluoride; Sf9, *Spodopetra frugiperda 9*.

axonal transport motor which conveys a particular group of membranous organelles distinct from those carried by kinesin heavy chain (KHC) or KIF3A/B proteins and different from synaptic vesicles and their precursors.

Materials and Methods

Construction and Transfection of Transfer Vector

Complete KIF2 cDNA, which was originally cloned into pUC19 (Aizawa et al., 1992), was reintroduced into pBluescript SK(+). A transfer vector was constructed using the pAcYM1 transfer vector (Matsuura et al., 1987) which contains the viral polyhedrin promoter for the expression of the cloned cDNA insert. The junction sites were sequenced and determined to contain ATG and the termination codons of KIF2.

The insect cell line *Spodopetra frugiperda* (Sf9) was propagated in TC100 medium (GIBCO BRL, Gaithersburg, MD) supplemented with bactotryptose broth and 10% fetal bovine serum (Summers and Smith, 1987). AcRP23.lacZ virus DNA (Kitts et al., 1990) was used because the replacement of the β-galactosidase gene by cDNA in the pAcYM1 vector can be detected in the presence of X-gal. Sf9 cells were transfected with mixtures of linearized AcRP23.lacZ DNA and pAcYM1/KIF2 by lipofection (lipofectin; GIBCO BRL) to generate recombinant baculovirus AcKIF2 containing KIF2 cDNA resulting from homologous recombination. The recombinant virus was purified by two rounds of screening in the presence of X-gal, and then grown to high titer stocks (10^7 plaque-forming U/ml) by serial amplification for the subsequent recombinant KIF2 expression.

Expression and Purification of KIF2

To purify the KIF2 protein, the Sf9 cell culture (30 ml) was resuspended 72 h after infection with 1/10 vol of PEM buffer (100 mM Pipes pH 6.8, 1 mM EGTA, 1 mM $MgCl_2$) containing 0.3 M sucrose, 1 mM DTT, 1 mM PMSF and 10 μg/ml leupeptin. The cells were homogenized and centrifuged at 100,000 *g* for 30 min at 4°C to obtain the crude extract. It was then supplemented with 100 μg/ml of taxol-stabilized purified microtubules, which were prepared as described before (Kondo et al., 1994), incubated at 20°C for 20 min and then centrifuged at room temperature (r.t.) for 15 min. This KIF2–microtubule pellet was resuspended with PEM buffer containing 10 mM Mg/ATP and centrifuged to wash out proteins derived from the Sf9 cells. KIF2 was then released from microtubules with the buffer containing 10 mM ATP and 100 mM NaCl. The resultant supernatant was considered as the purified KIF2 fraction, and contained about 150 μg/ml KIF2 at over 95% purity.

For the motility assay, KIF2 was further purified by loading the purified KIF2 fraction on a 5–20% linear sucrose density gradient. Fractions of 0.5 ml were collected and analyzed by SDS-PAGE.

Physical Properties of KIF2

KIF2's molecular weight was determined by the method described by Nangaku et al. (1994). Briefly Stoke's radius (R_s) of Sf9-expressed KIF2 was estimated by gel filtration on a Superose 6 column (Pharmacia, Piscataway, NJ) and calibrated with standard proteins: catalase, aldolase, bovine serum albumin, and ovalbumin. Sedimentation coefficients ($S_{20,w}$) were determined by centrifugation in a 5–20% sucrose density gradient using catalase, aldolase, bovine serum albumin, or ovalbumin as the internal standard.

Molecular Structure of KIF2

The recombinant KIF2-microtubule pellet was quick-frozen and deep-etched as described by Hirokawa et al. (1989). For rotary shadowing electron microscopy (EM), a 50-μl sample containing 1/10 vol of purified KIF2 fraction (final KIF2 concentration 15 μg/ml, ATP 1 mM, NaCl 10 mM) in 30% glycerol PEM buffer was sprayed on freshly cleaved mica flakes and processed as described by Hirokawa et al. (1989).

Motility Assay

Translocation of microtubules was observed according to procedures initially described by Vale et al. (1985). We used either fivefold diluted, purified KIF2 fraction containing 30 μg/ml of KIF2, 2 mM ATP, and 20 mM NaCl in PEM buffer, or fractions obtained after the sucrose density gradient centrifugation. Each sample (8 μl) was loaded onto a glass cover slip, and after 20 min of incubation the unadhered protein was removed and replaced with 5 μl of PEM buffer, 20 μM taxol, 5 mM MgATP, and 50 μg/ml of the taxol-stabilized microtubules or polarity-marked microtubules. Without removing the unadhered KIF2 protein, microtubules formed tight bundles in the solution, and it was impossible to observe the motility. Motility was monitored by video-enhanced differential interference contrast (DIC) microscopy as described by Kondo et al. (1994). Polarity-marked microtubules were prepared as described by Scholey et al. (1993).

Polyclonal and Monoclonal Antibody Production

Recombinant KIF2 was expressed in *Escherichia coli* (*E. coli*) using a PET3d vector with the full-length KIF2. Crude homogenate was loaded on SDS-PAGE and overexpressed KIF2 was cut out and electrically eluted from gels. After emulsification with Freund's adjuvant, the resultant compound was injected into rabbits and mice at doses of 0.5 and 0.1 mg, respectively. Rabbit serum was affinity purified with a KIF2-bound tripropyl Sepharose 6B column (Pharmacia).

Mouse spleen cells were fused with P3-653 myeloma cells using 50% polyethylene glycol 4000 (Kohler and Milstein, 1976). After limiting dilution and screening, hybridoma cultures were cloned that secreted antibodies against KIF2. Hybridoma cells were injected into peritoneal cavities of nude mice and accumulated ascites were collected and purified with a protein A–conjugated Sepharose column (Pharmacia).

Ligation of Mouse Peripheral Nerves and Immunostaining of Tissues

Saphenous nerves of 3-wk-old mice were tightly ligated under anesthesia (Hirokawa et al., 1990, 1991). After 20 h, the mice were transcardially perfused with 2% paraformaldehyde and 0.1% glutaraldehyde in 0.1 M phosphate buffer (pH 7.4). Small pieces of nerves both proximal and distal to the ligated portions were processed for light microscopy immunocytochemistry. Cerebellum was also similarly fixed by perfusion.

The ligated nerves were sectioned (10 μm) after cryoprotection by a cryostat. The sections were incubated with 10% normal goat serum in PBS. Next they were stained with affinity purified anti-KIF2 rabbit IgG (~10 μg/ml) for 60 min at r.t. Preimmune rabbit serum containing the same amount of IgG was used as a control. After washing, the sections were incubated with biotin-labeled anti-rabbit IgG goat IgG for 60 min, stained with horse radish peroxidase–labeled streptoavidin for 5 min, and then reacted with 3,3'-diaminobenzidine and hydrogen peroxide. They were mounted and observed with a Zeiss Axiophoto microscope.

Frozen tissue samples were sectioned on a cryostat, and preincubated with 5% skim milk in PBS. They were incubated with 25 μg/ml of anti-KIF2 monoclonal antibody or normal mouse IgG and then incubated with 1:100 rhodamine-labeled anti-mouse IgG second antibody.

Fractionation of Brain Tissue

Multiple fractions from 5-wk-old Wistar rat brain were prepared according to standard procedures (Fleicher and Pacer, 1974) with slight modifications (Nangaku et al., 1994). Briefly, brains from rats were gently homogenized with 3 ml of medium/gram of wet tissue. The composition of medium A included 0.32 M sucrose, 20 mM Tris-HCl, pH 7.6, and 3 mM $MgCl_2$. The homogenate was centrifuged at 700 *g* for 10 min at 4°C. This low-speed pellet was resuspended with 2.4 M sucrose buffer with 1 M $MgCl_2$, and then further centrifuged at 50,000 *g* for 60 min to yield a pellet of the nuclear fraction. The low-speed supernatant was centrifuged at 7,000 *g* for 10 min and subsequently centrifuged at 24,000 *g* for 10 min to yield a high-speed supernatant (S3) and pellet (P3). S3 was further centrifuged at 105,000 *g* for 100 min to yield a pellet of the microsomal fraction. By resuspending P3 in 10 ml of 0.25 M sucrose and centrifuging this suspension (24,000 *g* for 10 min), the mitochondrial fraction was recovered in pellet form.

Synaptic vesicles were at first prepared by the method of Ueda et al. (1979) (see Sato-Yoshitake et al., 1992) and then purified with permeation chromatography on controlled-pore glass (CPG 10 Polyol, 3000) (Huttner et al., 1983), while the growth cone fraction was prepared from 16-d-old embryonal mouse brain by the method of Pfenninger (1983) with slight modification (Ellis et al., 1985). Brain was placed in 0.32 M sucrose 1 mM Hepes buffer (pH 7.4) containing 1 mM $MgCl_2$, and then gently homogenized. After being centrifuged at 700 *g* for 15 min, the supernatant was loaded onto top of three layers of a discontinuous sucrose density; 0.75, 1.0,

and 2.6 M and spun to equilibrium for 60 min at 240,000 *g*. A, B, and C fractions were collected from the top of the interphase of different sucrose densities. The A fraction was further pelleted and slowly lysed with hypoosmic buffer containing 6 mM Tris/HCl (pH 8.2) with 0.5 mM EDTA. Membrane particles were collected by centrifugation at 80,000 rpm for 60 min using a Beckman TL100 rotor on a 1 M sucrose cushion.

Affinity Purification of Soluble and Membrane-associated KIF2

Three-day-old mouse brains were homogenized in PBS, then centrifuged at 100,000 *g* for 30 min at 4°C. the crude extract was loaded on an anti-KIF2 antibody-conjugated CNBr Sepharose 4B column (Pharmacia) and washed with PBS containing 1 M NaCl. The column was eluted by 0.1 M glycine (pH 2.2) and fractions were neutralized with 1 M Tris/HCl (pH 8.0).

Crude membrane fraction was prepared after centrifuging (100,000 rpm) the low-speed brain supernatant (S2) homogenized with a 0.32 M sucrose and 4 mM Hepes (pH 7.4) buffer containing 1 mM $MgCl_2$ and protease inhibitors. This membrane fraction was incubated for 30 min at r.t. with CNBr Sepharose beads conjugated with anti-KIF2 antibody, or normal mouse IgG, or with protein A-Sepharose beads conjugated via dimethylpimelumidate, with anti-synaptophysin antibody, or normal mouse IgG. The beads were washed with the same buffer, loaded on SDS-PAGE gels, and electrotransferred to PVDF membranes for immunoblotting. Beads were also processed for conventional EM.

Antibodies and Immunoblotting

The fractionated samples were separated by SDS-PAGE on 7.5 or 12.5% gels and transferred onto PVDF membranes. The sheets were reacted with affinity-purified polyclonal anti-KIF3A antibody, anti-kinesin monoclonal antibody (H2), or anti-KIF2 polyclonal antibody, followed by incubation with ^{125}I-protein A. The sheets were also reacted with antibodies against synaptic vesicle-related proteins including SV2, synaptophysin, synaptotagmin, synaptobrevin, and syntaxin (Buckley et al., 1985; Matthew et al., 1981; Baumert et al., 1989; Garcia et al., 1994).

Results

Biochemical Characterization and Purification of Recombinant KIF2

We used the baculovirus expression system as described by Kondo et al. (1994) to investigate the molecular characterization of KIF2. The Sf9-expressed, full-length KIF2 protein appeared as a band of about 100 kD (Fig. 1), being consistent with the predicted molecular weight (80,945 D) obtained from the nucleotide sequence (Aizawa et al., 1992). As indicated in Fig. 1 *A*, in the absence of ATP, KIF2 co-sedimented with taxol-stabilized microtubules assembled from pure tubulin. This binding was not significantly enhanced by the presence of AMP-PNP (Fig. 1 *A*, lane *2*), being a distinct property from that of kinesin and KIF3A (Kondo et al., 1994). KIF2 co-sedimented with microtubules was released from microtubules in the presence of 10 mM ATP and 100 mM NaCl (Fig. 1 *A*, lanes *12* and *16*). However, its amount in the supernatant was low when released by 10 mM ATP alone (Fig. 1 *A*, lanes *10* and *14*), and almost none when released by 100 mM NaCl alone (lanes *11* and *15*). This behavior suggests that KIF2 has two microtubule-binding sites, i.e., one ATP dependent and the other ATP independent.

We purified recombinant KIF2 by taking advantage of these biochemical properties, and Fig. 1 *B* shows the results. Briefly, KIF2 was co-sedimented with taxol-stabilized microtubules (Fig. 1 *B*, lane *5*), and this KIF2-microtubule pellet was washed with buffer containing 10 mM ATP (lane *7*). KIF2 was then released using buffer containing 10 mM ATP

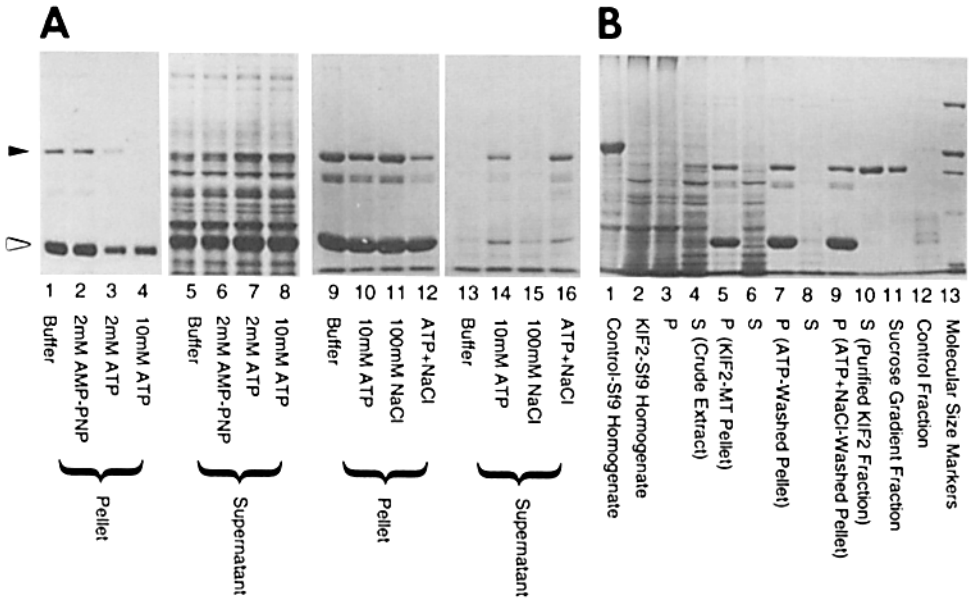

Figure 1. Biochemical characterization and purification of recombinant KIF2 protein. (*A*) Binding of KIF2 protein to microtubules. Crude extract from KIF2-expressing Sf9 cells was incubated with purified microtubules in buffer alone (lanes *1* and *5*), in buffer containing 2 mM AMP-PNP (lanes *2* and *6*), 2 mM ATP (lanes *3* and *7*), or 10 mM ATP (lanes *4* and *8*). The samples were centrifuged and the pellets (lanes *1–4*) and supernatants (lanes *5–8*) were separated on a 7.5% SDS-polyacrylamide gel and stained with Coomassie brilliant blue (CBB). To observe the release of KIF2 from microtubules, the KIF2-microtubule pellet (lane *1*) was further resuspended with buffer alone (lanes *9* and *13*), with buffer containing 10 mM ATP (lanes *10* and *14*), 10 mM NaCl (lanes *11* and *15*), or 10 mM ATP and 100 mM NaCl (lanes *12* and *16*). The samples were centrifuged again, and the pellets (lanes *9–12*) and supernatants (lanes *13–16*) were analyzed. The black arrowhead points to KIF2 and the white one to tubulin. (*B*) Purification profile of KIF2. Crude homogenate of KIF2-expressing Sf9 cells (lane *2*) was clarified by centrifugation (*P*, lane *3*; *S*, lane *4*). The supernatant (*Crude Extract*) was incubated with purified microtubules and centrifuged again (*P*, lane *5*; *S*, lane *6*). The resultant KIF2-microtubule pellet was washed with buffer containing 10 mM ATP (*P*, lane *7*; *S*, lane *8*). KIF2 was then released from microtubules by resuspending the pellet in buffer containing 10 mM ATP and 100 mM NaCl (*P*, lane *9*; *S*, lane *10*). For the motility assay, this supernatant (purified KIF2 fraction) was further purified by sucrose density gradient centrifugation (lane *11*). Samples from Sf9 cells infected with parent virus which did not express KIF2 were loaded on the same gel as controls (lane *1* corresponds to lane *2* and lane *12* to lane *10*, respectively). Lane *13* indicates the molecular size markers (200, 116, 97, 66, and 42 kD).

and 100 mM NaCl (lane *10*). At this stage, KIF2 appeared as a single band (>95% pure). For the motility assay, though, it was further purified by sucrose density gradient centrifugation (Fig. 1 *B*, lane *11*).

We estimated the molecular weight of recombinant KIF2 using $M\ (1\text{-}v r_{20,w}) = 6pR_S N_A S_{20,w}$. By gel filtration, R_S was estimated as 6.95 nm, while $S_{20,w}$ was determined to be 5.8S by sucrose density gradient centrifugation. Two trials gave the same value for R_S and $S_{20,w}$. The partial specific volume (v) was estimated as 0.73 from the amino acid composition (Zamyatnin, 1972). The molecular weight of KIF2 was subsequently calculated to be 171,000 D, which suggests it is a dimer since its predicted molecular weight obtained from the nucleotide sequence is 80,945 D.

Molecular Structure of Recombinant KIF2

The structure of purified KIF2 (Fig. 1 *B*, lane *10*) was initially observed by low-angle, rotary shadowing EM. As

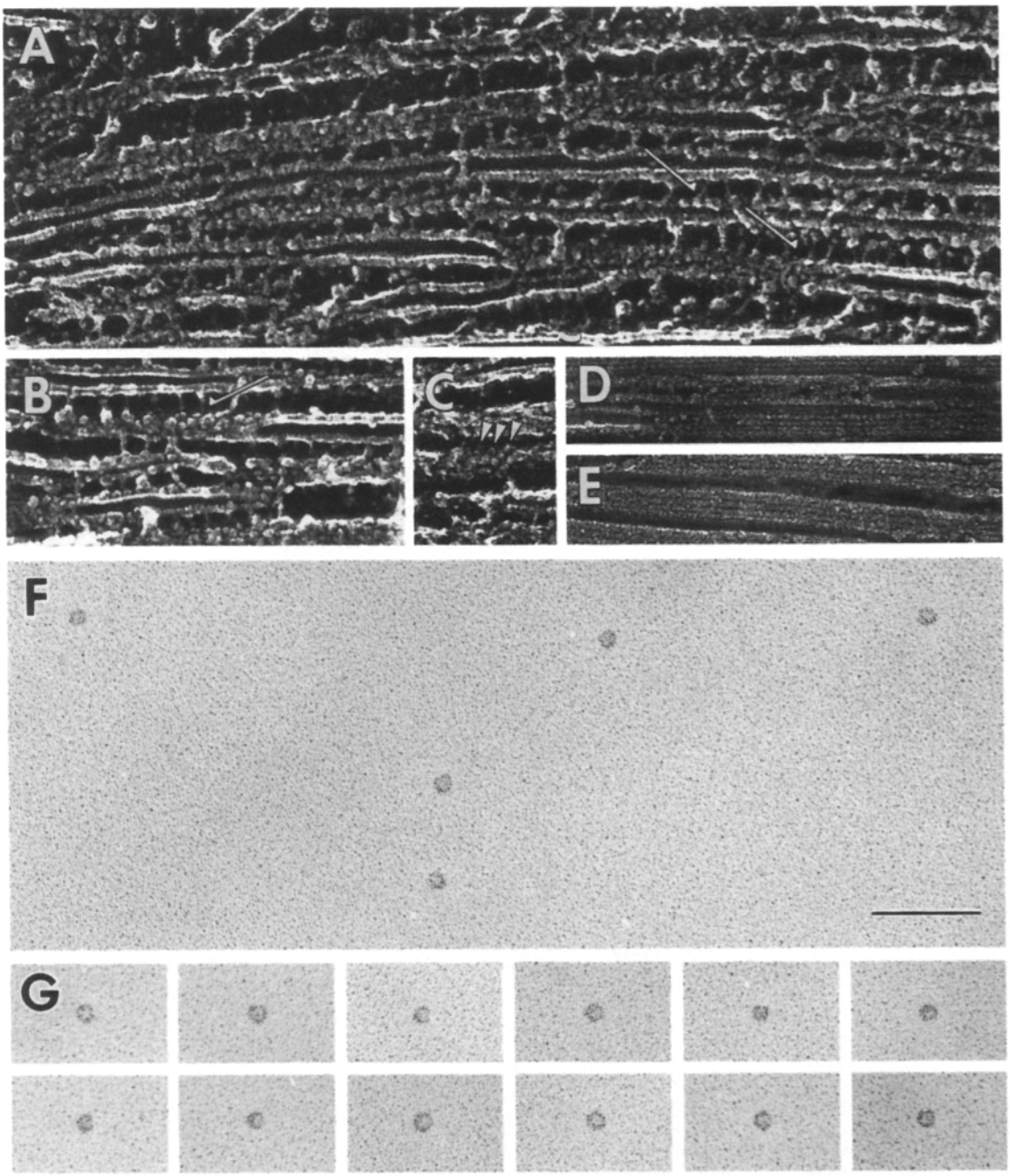

Figure 2. Molecular structure of recombinant KIF2 protein. (*A–E*) Electron micrographs showing quick-freeze, deep-etched microtubule pellets polymerized with KIF2 (*A–C*), with a control sample from Sf9 cells infected with parents virus (*D*) and with buffer alone (*E*). Numerous projections (*arrows*) and regular globular decorations (*arrowheads*) appear on the microtubules polymerized with KIF2 in *A–C*, while only tightly packed microtubules are observed in *D*. (*F* and *G*) Electron micrographs showing rotary shadowed KIF2. *F* shows a typical field, while a gallery of several representative molecules is shown in *G*. The molecules are similar in size and shape to the globular decorations observed in *A* and *C*. Bar, 100 nm.

shown in Fig. 2 (*F* and *G*) it appears as a globular molecule with a diameter of 16.4 ± 0.2 nm (n = 118). The diameter of each observed molecule was quite homogeneous, and was about 1.6 times bigger than the single head domains of kinesin and KIF3A (~10 nm) (Hirokawa et al., 1989; Kondo et al., 1994). Together with our biochemical data, this result suggests that KIF2 molecules exist mainly as dimer. The stalk domain could not be observed by this method, probably due to its instability without the presence of binding molecules.

Next we examined the microtubule pellet decorated with KIF2 (Fig. 1 *B*, lane *5*) by the quick-freeze deep-etch method, where short stalk domains were clearly visible (~17-nm long), being cross-linked to adjacent microtubules (Fig. 2, *A* and *B arrows*). Globular structures tended to decorate the surface of microtubules in a regular pattern (Fig. 2, *A* and *C*, *arrowheads*). They were similar in size and shape to the structures revealed by rotary shadowing EM, and adjoined one end of the stalk domain. From these data, we hypothesize that the unique NH_2-terminal region of the KIF2 protein may form a globular subdomain with the middle motor region, while the α-helical COOH-terminal region forms a short stalk domain.

Motor Activity of Recombinant KIF2

To prove KIF2 is a motor protein, a motility assay was performed with recombinant KIF2 protein in vitro as described by Kondo et al. (1994). The purified Sf9-expressed KIF2 fraction (Fig. 1 *B*, lane *10*) translocated purified microtubules on a glass surface at 0.47 ± 0.11 μm/s (n = 36). The similarly prepared fraction obtained from Sf9 cells infected with parent virus (Fig. 1 *B*, lane *12*) showed no motor activity indicating that this microtubule translocation activity is due to KIF2. Moreover, among the sucrose density gradient fractions, only the peak fractions (Fig. 1 *B*, lane *11*) translocated microtubules on the glass surface; thus clearly demonstrating that this motor activity is not caused by other Sf9-derived motor proteins, but solely by KIF2.

Polarity-marked microtubules were observed next. For this assay, purified tubulin was incubated with fragments of *Chlamydomonas* flagellar axonemes, producing a longer microtubule segment at the plus end and a shorter one at the minus end. As indicated in Fig. 3, all polarity-marked microtubules glided with their minus ends leading (n = 31), proving that KIF2 is a plus-end–directed microtubule-based motor protein.

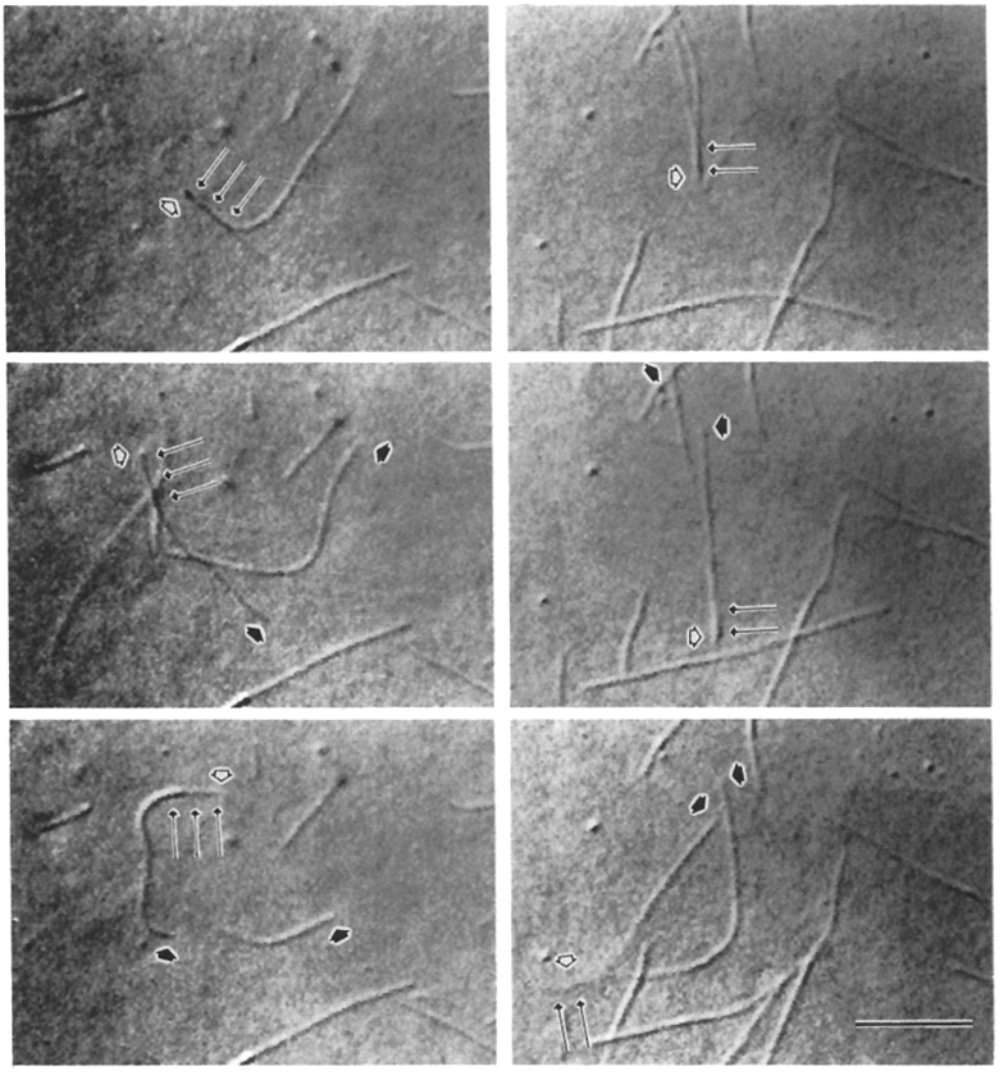

Figure 3. Movement of polarity marked microtubules on recombinant KIF2. Two series of video images taken at 30-s intervals are shown. Small arrows indicate the axoneme seed, white arrowheads the minus end of the seed, and black arrowheads the plus end of microtubules polymerized from the seed. The seeds are leading as microtubules translocate across the coverslip, indicating that KIF2 is a plus-end–directed motor protein. Bar, 5 μm.

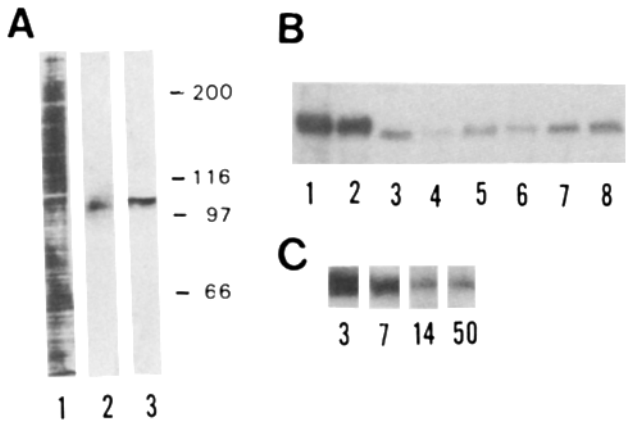

Figure 4. (*A*) Immunoblot analysis of the specificity of polyclonal and monoclonal antibodies. (Lane *1*) CBB staining of PVDF membrane of mouse total brain homogenate transferred on postnatal day 4 (P4). The same sheets were immunoblotted with anti-KIF2 polyclonal (lane *2*) and monoclonal (lane *3*) antibodies. Both antibodies bind specifically to KIF2 in total brain homogenate. (*B*) Western blot analysis of KIF2's tissue distribution. Each lane contains 1 mg of tissue total homogenate of mouse brain at P4. Lane *1*, cerebrum; lane *2*, cerebellum; lane *3*, lung; lane *4*, liver; lane *5*, kidney; lane *6*, heart; lane *7*, spleen; lane *8*, thymus. KIF2 is predominantly expressed in brain and at a minor level in other tissues. (*C*) Western blot analysis of KIF2's developmental expression in mouse brain. Each lane contains 2 mg of total brain homogenate at P3, P7, P14, and P50. KIF2 is abundant in younger brain (P3 ~ P7).

Western Blot Analysis of KIF2's Distribution

We raised polyclonal and monoclonal antibodies to recombinant KIF2, and both specifically bound to KIF2 in the mouse total brain homogenate (Fig. 4 *A*). Using affinity-purified polyclonal antibody, we analyzed the tissue distribution and developmental expression of KIF2 by immunoblotting (Fig. 4, *B* and *C*), where KIF2 was abundantly present in the whole brain, less so in the spleen and thymus, much less so in the lung, while faint bands were detected in all the other tissues (Fig. 4 *B*). The amount of most KIF2 expressed in the brain decreased postnatally, and only a little was detected in adult brain (Fig. 4 *C*). These data indicate that KIF2 is dominantly expressed in the young nervous system of mice in spite of its ubiquitous existence in all tissues.

Immunocytochemical Analysis of KIF2

We examined KIF2's developmental localization in various regions of the mouse central nervous system, and it was found to be transiently expressed in postmitotic young neurons, especially in developing axons. In the cerebellum where the tissues develop postnatally, KIF2 showed peak expression at P7. As shown in Fig. 5, at P7, parallel fibers located in molecular layer were stained most intensely, in addition to the occurrence of dot-like staining of the granular cells' cell bodies and synapses from mossy fibers. The Purkinje cells' axons present in the white matter should also be noted. However, the external granular layer was not stained, which consists of neuroprecursor cells formed during or just after mitosis. Staining of the molecular layer faded out from inner side (Fig. 5, *asterisk*) at P14, which was coordinated with the termination of axonal growth, and became very weak in the adult cerebellum (data not shown). Simultaneously, staining of the white matter also vanished. In the olfactory bulb, where neurite outgrowth persists for life, staining did not decrease in adult tissue (data not shown).

Localization of KIF2 in Ligated Peripheral Nerves

Since recombinant KIF2 was found to be a plus-end–directed microtubule-based motor in vitro (Fig. 3), and corresponding staining of axons occurred in vivo (Fig. 5), this protein must play some role in axonal transport. To elucidate KIF2's dynamics within axons, we observed its localization after ligating the peripheral (saphenous) nerves of adult mice. Our previous research has demonstrated that anterogradely and retrogradely transported membranous organelles, respectively, accumulate at the proximal and distal region of the

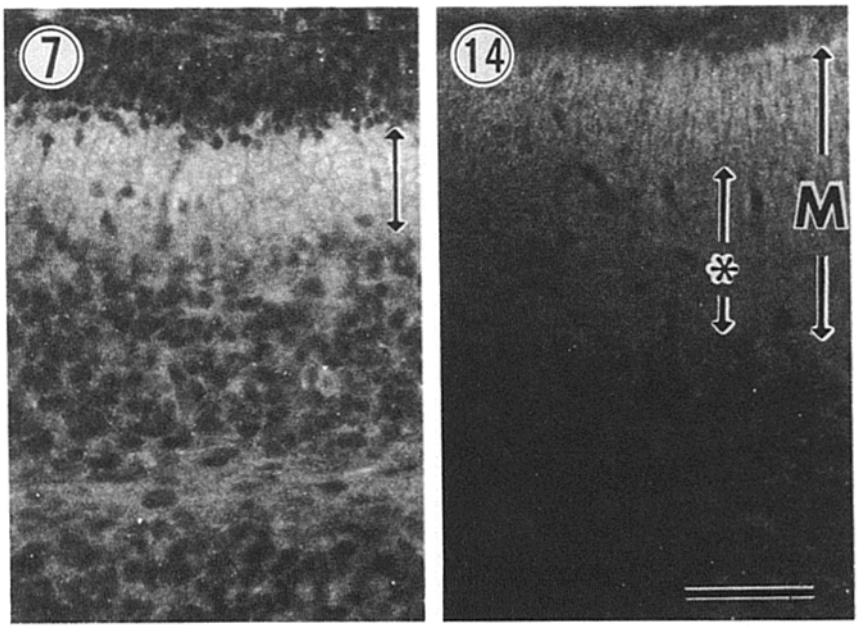

Figure 5. Immunofluorescence micrographs of developing cerebellum. Numbers indicate the postnatal days. Intense staining of molecular layer at P7 dramatically diminished from the inner side at P14 (*asterisk*, inner side of the molecular layer). *M*, molecular layer. Bar, 100 μm.

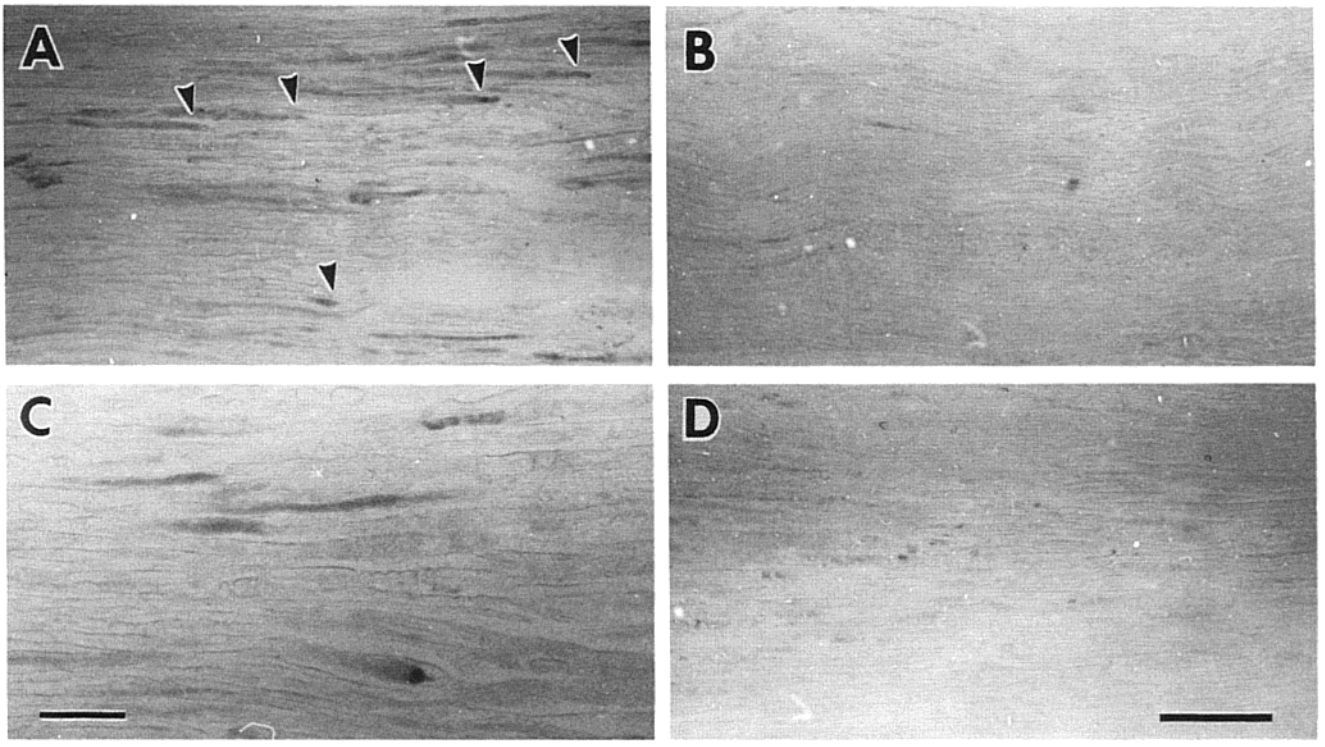

Figure 6. Immunofluorescence micrographs of the ligated nerves with anti-KIF2 antibody. (*A*) Proximal region. (*B*) Distal region of the ligated portion. The right side of *A* and left side of *B* are near the ligated portion, with about 450 μm of separation. (*C*) Higher magnification of the proximal region. (*D*) Control of proximal region stained with normal rabbit IgG as the first antibody. Arrowheads indicate the accumulation of KIF2. Bars: (*A*, *B*, and *D*) 100 μm; 50 μm (*C*).

ligated portion (Hirokawa et al., 1990, 1991). After 20 h of ligation, the KIF2 polyclonal antibody strongly stained the proximal region, though much less so the distal one (Fig. 6 *A*, arrowheads). Higher magnification showed staining in the axonal cytoplasm, where the storage of membranous organelles increased the diameter (Fig. 6 *C*). Although we had observed the accumulation of kinesin and KIF3A in 6-h ligated nerves, we could not detect KIF2 after 6 h of ligation. We surmise it is due to smaller volume of KIF2 in the adult peripheral nerves compared to those of kinesin and KIF3A (unpublished data). In addition, we noticed that in case of KIF2, compared to kinesin (Hirokawa et al., 1991) and KIF3A (Kondo et al., 1994), the accumulated regions tended to be more distant from the ligated portions.

Subcellular Localization of KIF2

Because KIF2 was co-localized with membranous organelles during axonal anterograde transport, we further investigated its intracellular compartment by subcellular fractionation. In contrast to kinesin and KIF3A, which are diffusely distributed in all fractions, KIF2 was relatively concentrated in the microsome and crude synaptic vesicle fractions, whereas not so in the cytosol (Fig. 7 *A*). Since KIF2 was abundantly expressed in the juvenile neurons during axonal growth, we isolated growth cones according to Pfenninger's method (1983) (Ellis et al., 1985). Western blotting results showed it to be packed in growth cone particles in embryonal brain, and that it mainly associates with the membrane fraction after hypo-osmic lysis of growth cones (Fig. 7 *B*).

Affinity Purification of KIF2

To further investigate the subpopulation of membranous organelles associated with KIF2, we immunologically isolated them. The soluble fraction from crude brain extract was initially purified in an anti-KIF2 monoclonal antibody–conjugated Sepharose column, and the eluted fraction contained a single band of KIF2, but included no associated protein such as a light chain (Fig. 8 *A*). Next, membrane-associated KIF2 was isolated by immunoprecipitation with anti-KIF2 antibody-conjugated Sepharose beads. The total brain homogenate at P3 was then centrifuged twice at low and high speeds. The high-speed pellet was resuspended and reacted with antibody-conjugated beads, with EM showing relatively uniform vesicles (100–120-nm diam) located on the surface of the beads (Fig. 9 *A*, *arrowheads*), while none being present on the normal IgG-conjugated ones (Fig. 9 *B*); hence, indicating KIF2 immunoprecipitated in membrane bound form. At higher magnification, vesicles are mostly uniform in size (100–120 nm), and sometimes partial multivesicular bodies were also observed, consistent with its existence in growth cones. This suggests a possibility that some population of partial multivesicular bodies are conveyed anterogradely in the axon. In fact we observe a small population of small multivesicular bodies in the proximal region of the ligated axons (see Fig. 3 *A* in Hirokawa et al., 1990).

Immunoblotting of this beads fraction definitely showed that these membranous organelles are associated with KIF2, but that they are different from kinesin- or KIF3A-binding ones (Fig. 8 *B*). We also tried to detect KIF4-bound mem-

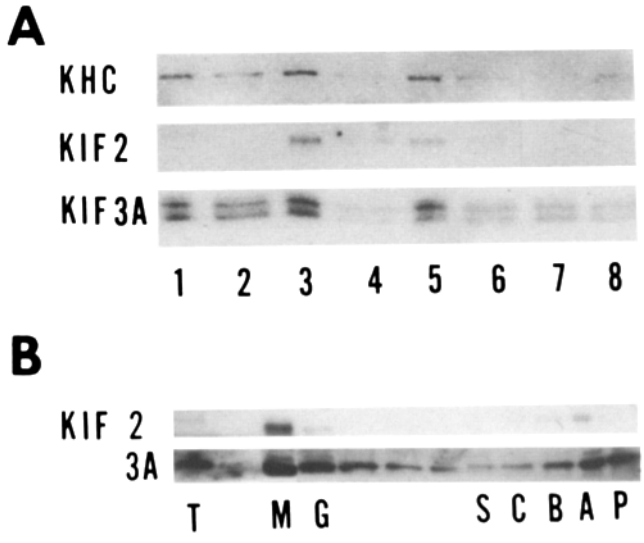

Figure 7. Immunoblot analysis of subcellular fractionation. (*A*) Subcellular fractions obtained from 5-wk-old rat brain. A 20 μg of sample was loaded on each lane. Lane *1*, crude homogenate; lane *2*, cytosol fraction; lane *3*, microsomal fraction; lane *4*, mitochondrial fraction; lane *5*, synaptic vesicle fraction; lane *6*, nuclear fraction. KIF2 is relatively concentrated in microsomal and synaptic vesicle fractions. (*B*) Purification process of growth cone particles from mouse embryonal brain. Low-speed supernatant of embryonal brain was loaded on a discontinuous sucrose densities (*P*, preloaded supernatant) and S, A, B, C fractions were obtained (*S*, 0.32 M sucrose fraction, corresponding to the cytosol fraction; *A*, *B*, *C*, boundary fraction between 0.32 and 0.75 M, 0.75 and 1.0 M, and 1.0 and 2.7 M sucrose buffer, respectively). The A fraction, corresponding to the growth cone particles, was further pelleted down by centrifugation (fraction G) and lysed by hypo-osmic shock, then centrifuged again on a 1 M sucrose cushion to obtain a membranous fraction as a pellet (fraction M). (*T*) total brain homogenate. Note KIF2 is concentrated in the membrane fraction of the growth cones.

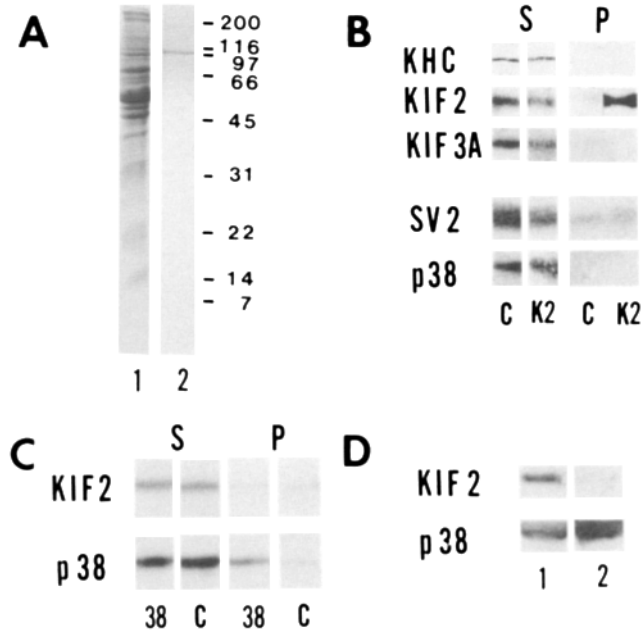

Figure 8. Affinity purification of soluble and membrane-bound KIF2 (*A*) Affinity purification of soluble KIF2. (Lane *1* and *2*) CBB staining of preload supernatant (crude extract of P3 mouse brain) (lane *1*) and eluted fraction (lane *2*). Eluted fraction contains only KIF2. No associated protein is present. (*B*) Immunoblot analysis of KIF2-associated vesicles isolated by immunoprecipitation with anti-KIF2 monoclonal antibody. The crude membrane fraction was incubated with anti-KIF2 antibody lanes *K2*) or normal mouse IgG (lanes *C*) conjugated beads. Supernatants (lanes *S*) and pellets (lanes *P*) were recovered by sedimentation and loaded on SDS-polyacrylamide gel and transferred to PVF membrane for immunoblot with anti-kinesin, KIF2, KIF3A, SV2, and synaptophysin antibodies. KIF2-associated vesicles include neither kinesin, KIF3A, SV2, nor synaptophysin. (*C*) Immunoblot analysis of synaptophysin-associated vesicles isolated by immunoprecipitation. Supernatants (lane *S*) and pellets (lane *P*) after being incubated with anti-synaptophysin (lanes *38*) and normal mouse IgG (lanes *C*) conjugated beads were immunoblotted with anti-KIF2 and synaptophysin antibodies. (*D*) Immunoblot analysis of crude (lane *1*) and pure synaptic vesicle fraction (lane *2*) with anti-KIF2 and synaptophysin antibodies. KIF2 did not concentrate in the synaptic vesicles purified with CPG column.

branous organelles, but we could not, because of its lower expression level at this developmental stage. KIF4 was found to be expressed abundantly at earlier stages than KIF2 (data not shown).

Although subcellular fraction data indicates KIF2's abundance in the crude synaptic vesicle fraction, membrane markers of the synaptic vesicles, i.e., synaptophysin and SV2, were not associated with KIF2 binding vesicles (Fig. 8 *B*). In addition, other synaptic vesicle-related proteins including synaptotagmin, synaptobrevin, and synataxin were not concentrated in this KIF2-associated beads fraction (data not shown). Immunoprecipitation of vesicles with anti-synaptophysin antibody also failed to detect KIF2 in the synaptophysin-associated beads fraction (Fig. 8 *C*). Further purification of crude synaptic vesicle fraction by CPG column enabled KIF2 bound membrane fraction to separate from pure synaptic vesicles fraction concentrated in synaptophysin (Fig 8 *D*). This finding is of particular interest because even though vesicles associated with KIF2 are contained in the so-called synaptic vesicle fraction, they are distinct in nature from synaptic vesicles.

Discussion

We have elucidated KIF2's biochemical behavior, molecular structure, motor activity, and cellular/subcellular distribution. Our results indicate the following: (*a*) KIF2 has an ATP-dependent microtubule binding site and exists as a dimer without a light chain; (*b*) KIF2 translocates microtubules in vitro as a plus-end–directed motor at a velocity two thirds that of kinesin; (*c*) KIF2 is abundant in growing axons; (*d*) KIF2-associated vesicles accumulate in the proximal region of ligated nerves; and (*e*) immunologically isolated KIF2-binding vesicles are different from those associated with kinesin, KIF3A, and synaptic vesicle markers. These data strongly suggest KIF2 is a new microtubule-based motor which carries a particular population of vesicles in fast anterograde axonal transport.

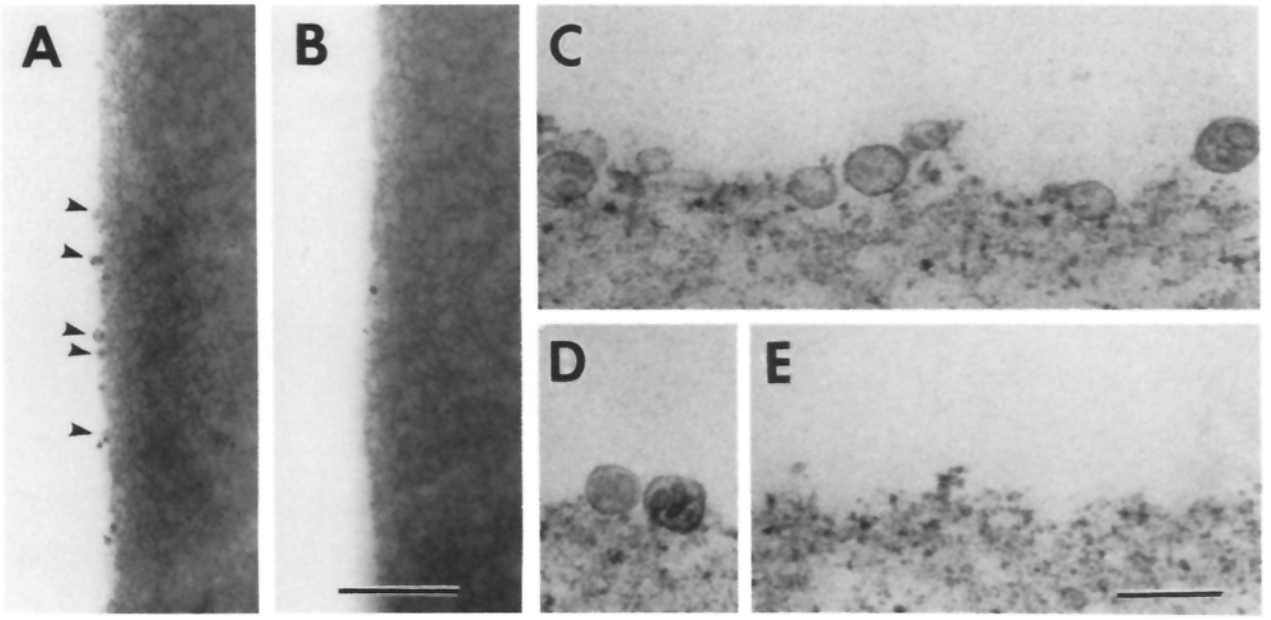

Figure 9. Electron micrographs of affinity purified KIF2-associated vesicles. The surface of anti-KIF2 antibody-conjugated (*A*, *C*, and *D*) or normal mouse IgG conjugated beads (*B* and *E*) after being incubated with the crude membrane fraction. At lower magnification, membranous organelles were visible on the anti-KIF2 antibody conjugated bead (*A*, *arrowheads*), but not on the normal mouse immunoglobulin conjugated one (*B*). Higher magnification (*C*, *D*, and *E*) showed KIF2-associated vesicles are observed as relatively uniform particles with a diameter of 100–120 nm. Multivesicular bodies are also found. Bars: (*A* and *B*) 2 μm; (*C*, *D*, and *E*) 200 nm.

KIF2 Has a Unique Structure Distinct from Kinesin

The primary structure of KIF2 has a conserved motor domain at the center of the molecule, being different from that located at the NH_2 terminus in conventional kinesins and that at the COOH terminus in other groups of kinesin-like proteins such as KAR3 and ncd (Meluh et al., 1990; Mcdonald and Goldstein, 1990; Endow et al., 1990). Sf9-expressed recombinant KIF2, similar to kinesin, exists as a homodimer, binds microtubules in a ATP-dependent manner, and translocates microtubules as a plus-end-directed motor. However, analysis of its submolecular structure by low-angle rotary shadowing EM and the quick-freeze deep-etch method showed it consists of a single large globular domain (16.4 ± 0.2 nm) and has a short stalk domain which could only be observed by the latter method. KIF2's NH_2-terminal structure may contribute to the formation of this bigger globular domain with motor domain, producing a structure totally unique from other kinesin-like proteins. Moreover, the absence of a light chain also contradicts conventional structural patterns. Its biochemical properties suggest the presence of another microtubule binding site which is ATP independent and which enables it to cross-bridge between microtubules and bundle them as observed in the quick-freeze samples. On the other hand, no evidence exists that KIF2 bundles microtubules in vivo, instead moving along microtubules: hence, suggesting this phenomenon may only be observed in vitro and is not physiological. Immunoprecipitation of native KIF2 in soluble fractions using anti-KIF2 antibodies showed it has no associated protein like kinesin's light chain. Because our immunoprecipitation results using antibody-labeled beads revealed that KIF2 binds to a particular population of small vesicles, its tail domain is likely to function in vitro as a binding site for associated vesicles rather than microtubules. Although this new protein shows a unique structure distinct from kinesin and other KIFs, the ubiquitous distribution and existence of new homologues such as CHO26 and DFLP1 (Sekine et al., 1994; Wordeman et al., 1995) suggest it may be a new family which plays a fundamental role regarding species and tissues.

KIF2 Functions in Growing Axons in the Nervous System

KIF2 is dominantly expressed in the nervous system of mice, especially in juvenile brain, though it is expressed in all tissues (Fig. 4, *B* and *C*). Its continuous existence in olfactory bulbs, where neuite outgrowth and plasticity persist for life (Graziadei et al., 1979), also supports its function in the developing brain. Immunocytochemistry of the cerebellum showed that KIF2 is abundant in growing axons, and was condensed in parallel fibers of granular cells on postnatal day 7 (P7), disappearing from the inner side at P14, similar to MAP1B (Schoenfeld et al., 1989; Sato-Yoshitake et al., 1989) (Fig. 5). Subcellular fractionation of embryonal brain also demonstrated KIF2's abundance in growth cones (Fig. 7 *B*). Concerning KIF2's function in vivo, two possibilities exist: (*a*) in the juvenile brain, KIF2 transports an abundant cargo; and (*b*) KIF2's cargo exists in all stages of nervous system development, being succeeded to be transported by another motor appearing at a later stage. Western blotting analysis showed that KIF2 still exists in adult brain, though its level is close to the sensitivity of immunocytochemistry. Our PCR cloning has not yet led to discovering another protein which is similar to KIF2 and becomes a counterpart in adult

brain, and therefore, possibility (*a*) is considered most probable. We expect that quantitative identification will ultimately shed light on this question.

KIF2-associated Vesicles Are Different from Synaptic Vesicles

KIF2 exists in membrane-bound form rather than in soluble form in vivo (Fig. 7). When we isolated KIF2-associated membranous organelles by the immunological method, they were found to be free of other motors such as kinesin and KIF3A (Fig. 8), being transported anterogradely in axons (Fig. 6). This behavior suggests that they are only conveyed by KIF2 which is abundant in developing brain. Moreover, subcellular fractionation also showed these vesicles to be distributed differently from kinesin and KIF3A (Fig. 8). Although we have not isolated kinesin- or KIF3A-associated vesicles, this data suggests a possibility that some motors exist which convey specific cargo. Previous data on a kinesin mutant (Gho et al., 1992), which apparently did not influence synaptic vesicle concentration, and unc-104 (Otsuka et al., 1991), a putative kinesin-like motor specific for synaptic vesicles, support this possibility.

KIF2 is relatively concentrated in the synaptic vesicle fraction, as well as in the microsomal one (Fig. 7). Subcellular fractionation of embryonal mouse brain also showed its abundance in growth cones in membrane-bound form, which resembles synaptophysin and SV2, both membrane markers of synaptic vesicles. However, on the contrary, developmental regulation separates KIF2 from synaptophysin and SV2. The distribution pattern of accumulated KIF2 in the proximal region of ligated nerves is also atypical (Fig. 6), compared with other KIFs (Hirokawa et al., 1991; Kondo et al., 1994), and differs from that of synaptophysin and SV2 (data not shown) since the accumulated portion tended to be more distant from the ligated region. EM indicated that the diameter of KIF2-associated vesicles is between 100–120 nm, different from typical synaptic vesicles (Fig. 9), while immunoprecipitation of KIF2-associated vesicles and purification of synaptic vesicles by CPG column clearly show that they are distinct from synaptic vesicles and their precursors (Mundigl et al., 1993; Feany et al., 1993).

The identification of axonal transport motors enables researchers to clarify and differentiate the transport mechanism carried by each motor. We expect that the presented results will provide the foundation for discovering functional diversity and redundancy of the motor proteins in the nervous system. Future work will be directed at examining the co-localization of other membrane markers with KIF2-associated vesicles, and hopefully this will reveal KIF2's specific function in the nervous system.

Sincere gratitude is extended to Dr. Y. Matsuura (Laboratory of Hepatitis Viruses, Department of Virology II, National Institutes of Health, Bethesda, MD) for his valuable technical advice concerning the baculovirus system, to Dr. S. Karaki and Dr. S. Fujita for technical advice about the monoclonal antibody system. We also thank Dr. K. Yoshimura (Zoological Institute, Faculty of Science, University of Tokyo, Tokyo, Japan) for his technical advice and generous gift of the *Chlamydomonas*, Dr. M. Suffines (National Cancer Institute) for supplying the taxol; Drs. G. S. Bloom (University of Texas, Southwestern Medical Center, Dallas, TX), K. M. Buckley, R. Kelley, R. Jahn, L. F. Reichardt, and P. De Camilli for their kind gifts of antibodies; Drs. Y. Okada, A. Harada, S. Okabe, H. Yamazaki, and H. Ohnishi for technical advice and assistance; Mr. F. Ishidate (Carl Zeiss, Tokyo, Japan) for assistance with the light microscopy; and Ms. Y. Kawasaki and Ms. H. Sato for their secretarial assistance.

This work was supported by a special Grant-in-Aid for Scientific research from the Ministry of Education, Science and Culture of Japan, and a grant from RIKEN to N. Hirokawa.

Received for publication 23 August 1994 and in revised form 23 November 1994.

References

Aizawa, H., Y. Sekine, R. Takemura, Z. Zhang, M. Nangaku, and N. Hirokawa. 1992. Kinesin family in murine central nervous system. *J. Cell Biol.* 119:1287–1296.

Baumert, M., P. R. Maycox, F. Navone, P. Decamilli, and R. Jahn. 1989. Synaptobrevin an integral membrane protein of 18,000 daltons present in small vesicles of rat brain. *EMBO (Eur. Mol. Biol. Organ.) J.* 8:379–384.

Brady, S. T. 1985. A novel brain ATPase with properties expected for the fast axonal transport motor. *Nature (Lond.).* 317:73–75.

Buckley, K., and R. B. Kelly. 1985. Identification of a transmembrane glycoprotein specific for secretory vesicles of neuronal and endocrine cells. *J. Cell Biol.* 100:1284–1294.

Dahlström, A. B., A. J. Czernik, and Jia-Yi Li. 1992. Organelles in fast axonal transport. *Mol. Neurobiol.* 92:157–177.

Ellis, L., I. Wallis, E. Abreu, and K. H. Pfenninger. 1985. Nerve growth cones isolated from fetal rat brain, IV. Preparation of a membranous subfraction and identification of a membrane glycoprotein expressed on sprouting neurons. *J. Cell Biol.* 101:1977–1989.

Endow, S. A., S. Henikoff, and L. S. Niedziela. 1990. Medication of meiotic and early mitotic chromosome segregation in Drosophila by a protein related to kinesin. *Nature (Lond.).* 345:81–83.

Feany M. B., A. G. Yee, M. L. Delvy, and K. M. Buckley. 1993. The synaptic vesicle proteins SV2, synaptotagmin and synaptophysin are sorted to separate cellular compartments in CHO fibroblasts. *J. Cell Biol.* 123:575–584.

Fleichner, S., and L. Packer. 1974. Biomembranes, Part A. *Methods Enzymol.* Vol. 31.

Garcia, E. P., E. Gatti, M. Butler, J. Burton, and P. De Camilli. 1994. A rat brain sec1 homologue related to rop and unc 18 ineracts with syntaxin. *Proc. Natl. Acad. Sci. USA.* 91:2003–2007.

Gho, M., K. McDonald, B. Ganetzky, and W. M. Saxon. 1992. Effects of kinesin mutations on neural functons. *Science (Wash. DC).* 258:313–316.

Goldstein, L. S. B. 1993. With apologies to Scheherazade: tales of 1001 kinesin motors. *Annu. Rev. Genet.* 27:319–351.

Grafstein, B., and D. S. Forman. 1980. Intracellular transport in neurons. *Physiol. Rev.* 60:1167–1283.

Graziadei, P. P. C., and G. A. M. Graziadei. 1979. Continuous nerve cell renewal in the olfactory system. *J. Neurocytol.* 8:1–18.

Hirokawa, N. 1982. Cross-linker system between neurofilaments, microtubules, and membranous organelles in frog axons revealed by the quick-freeze, freeze-fracture, deep-etching method. *J. Cell Biol.* 94:129–142.

Hirokawa, N., K. K. Pfister, H. Yorifuji, M. C. Wagner, S. T. Brady, and G. S. Bloom. 1989. Submolecular domains of bovine brain kinesin identified by electron micorscopy and monoclonal antibody decoration. *Cell.* 56: 867–878.

Hirokawa, N., R. Sato-Yoshitake, T. Yoshida, and T. Kawashima. 1990. Brain dynein (MAP1C) localizes on both anterogradely and retrogradely transported membranous organelles. *J. Cell Biol.* 111:1027–1037.

Hirokawa, N., R. Sato-Yoshitake, N. Kobayashi, K. K. Pfister, G. S. Bloom, and S. T. Brady. 1991. Kinesin associates with anterogradely transported membranous organelles in vivo. *J. Cell Biol.* 114:295–302.

Hirokawa, N. 1991. Molecular architecture and dynamics of the neuronal cytoskeleton. *In* Neuronal Cytoskeleton. R. D. Burgoyne, editor. Wiley-Liss, Inc., New York. 5–74.

Huttner, W. B., W. Chiebler, P. Greengard, and P. De Camilli. 1983. Synapsin I (Protein I), a nerve terminal-specific phosphoprotein. III. Its association with synaptic vesicles studied in a highly purified synaptic vesicle preparation. *J. Cell Biol.* 96:1374–1388.

Kitts, P. A., M. D. Ayres, and R. D. Possee. 1990. Linearization of baculovirus DNA enhances the recovery of recombinant virus expression vectors. *Nucleic Acids Res.* 18:5667–5672.

Kohler, G., and C. Milstein. 1976. Derivation of specific antibody-producing tissue culture and tumor lines by cell fusion. *Eur. J. Immunol.* 6:511–519.

Kondo, S., R. Sato-Yoshitake, Y. Noda, H. Aizawa, T. Nakata, Y. Matsuura, and N. Hirokawa. 1994. KIF3A is a new microtubule-based anterograde motor in the nerve axon. *J. Cell Biol.* 125:1095–1107.

Matsuura, Y., R. D. Posse, H. A. Overton, and D. H. L. Bishop. 1987. Baculovirus expression vector: the requirement for high level expression of proteins, including glycoproteins. *J. Gen. Virol.* 68:12338-1250.

Matthew, W. D., L. Tsavaler, and L. F. Rechardt. 1981. Identification of a synaptic vesicle-specific membrane protein with a wide distribution in neuronal and neurosecretory tissue. *J. Cell Biol.* 91:257–269.

Mcdonald, H. B., and L. S. B. Goldstein. 1990. Identification and characterization of gene encoding a kinesin-like gene in Drosophila. *Cell.* 61:991–1000.

Meluh, P. B., and M. D. Rose. 1990. KAR3, a kinesin-related gene required for yeast nuclear fusion. *Cell.* 60:1029–1041.

Mundigl, O., M. Matteoli, L. Daniell, A. Thomas-Reetz, A. Metcalf, R. Jahn, and P. De Camilli. 1993. Synaptic vesicle proteins and early endosomes in cultured hippocampal neurons: differential effects of Brefeldin A in axons and dendrites. *J. Cell Biol.* 122:1207–1221.

Nangaku, M., R. Sato-Yoshitake, Y. Okada, Y. Noda, R. Takemura, H. Yamazaki, and N. Hirokawa. 1994. KIF1B: a new microtubule plus-end directed motor for mitochondria transport. *Cell.* In press.

Otsuka, A. J., A. Jeyaprakash, J. Garcia-Anpveros, L. Z. Tang, G. Fisk, T. Hartshorne, R. Franco, and T. Born. 1991. The *C. elegans* unc-104 gene encodes a putative kinesin heavy chain-like protein. *Neuron.* 6:113–122.

Paschal, B. M., and R. B. Vallee. 1987. Retrograde transport by the microtubule associated protein MAP1C. *Nature (Lond.).* 330:181–183.

Pfenninger, K. H., L. Ellis, M. P. Johnson, L. B. Friedman, and S. Somlo. 1983. Nerve growth cones isolated from fetal rat brain: subcellular fractionation and characterization. *Cell.* 35:573–584.

Sato-Yoshitake, R., Y. Shiomura, H. Miyasaka, and N. Hirokawa. 1989. Microtubule-associated protein 1B: molecular structure, localization, and phosphorylation dependent expression in developing neurons. *Neuron.* 3:229–238.

Sato-Yoshitake, R., H. Yorifuji, M. Inagaki, and N. Hirokawa. 1992. The phosphorylation of kinesin regulates its binding to synaptic vesicles *J. Biol. Chem.* 267:23930–23936.

Schoenfeld, T. A., L. McKerracher, R. Obar, and R. B. Vallee. 1989. MAP 1A and MAP 1B are structurally related microtubule associated proteins with distinct developmental patterns in the CNS. *J. Neurosci.* 9:1712–1730.

Scholey, J. M. 1993. Motility Assays for Motor Proteins. Academic Press, San Diego, CA.

Sekine, Y., Y. Okada, Y. Noda, S. Kondo, H. Aizawa, R. Takemura, and N. Hirokawa. 1994. A novel microtubule-based motor protein (KIF4) for organelle transports, whose expression is regulated developmentally. *J. Cell Biol.* 127:187–201.

Summers, M. D., and G. E. Smith. 1987. A manual of methods of baculovirus vectors and insect cell culture procedures. Texas Agriculture Experiment Station Bull. No. 1555.

Ueda, T., P. Greengard, K. Berzins, R. S. Cohen, F. Blomberg, D. J. Grab, and P. Siekevitz. 1979. Subcellular distribution in cerebral cortex of two proteins phosphorylated by a cAMP-dependent protein kinase. *J. Cell Biol.* 83:308–319.

Vale, R. D., B. L. Schnapp, T. S. Reese, and M. S. Sheetz. 1985. Organelle, bead, and microtubule translocation promoted by soluble factors from squid giant axons. *Cell.* 40:559–569.

Wordeman, L., and T. J. Mitchison. 1995. Identification and particle characterization of mitotic centromere-associated kinesin, a kinesin-related protein that associates with centromeres during mitosis. *J. Cell Biol.* 128:95–105.

Zamyatnin, A. A. 1972. Protein volume in solution. *Prog. Biophys. Mol. Biol.* 24:107–123.